JOC The Journal of Organic Chemistry

Article

pubs.acs.org/joc

Carbonyl-Twisted 6-Acyl-2-dialkylaminonaphthalenes as Solvent Acidity Sensors

Amy M. Green, Hannah R. Naughton, Zachariah B. Nealy, Robert D. Pike, and Christopher J. Abelt*

Department of Chemistry, College of William and Mary, Williamsburg, Virginia 23187-8795, United States

Supporting Information

ABSTRACT: Derivatives of 2-propionyl-6-dimethylaminonaphthalene (PRODAN) with twisted carbonyl groups were investigated as highly responsive sensors of H-bond donating ability. The PRODAN derivative bearing a pivaloyl group (**4**) was prepared. The torsion angle between the carbonyl and naphthalene is 26° in the crystal. It shows solvatochromism that is similar to five other PRODAN derivatives (**1**−**3**, **5**, **6**). Twisted-carbonyl derivatives **3**, **4**, and **6** show strong fluorescence quenching in protic solvents. The order of magnitude of the quenching is linearly related to the H-bond donating ability of the solvent (SA) but not to other solvent properties. Binary mixtures of protic solvents show specific interaction effects with respect to quenching and solvatochromism. Aggregation in water is an issue with the pivaloyl derivatives.

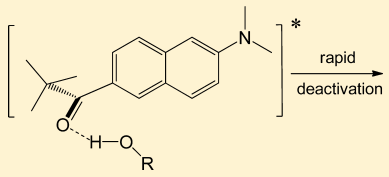

INTRODUCTION

Molecular sensors function by interrogating a targeted environment. The development of sensors for materials and biological systems is an important area of research. Sensors must respond to an environmental stimulus with a quantifiable signal.[1] Fluorescent compounds are particularly useful as sensors when their emission is modulated by the nature of their immediate surroundings. The interaction between the excited molecule and its environment can affect the fluorescence intensity, emission wavelength maximum and lifetime.

PRODAN (6-propionyl-2-dimethyaminonaphthalene, **1**, Figure 1) is a well-known fluorophore that serves as a chemosensor of micropolarity. It was prepared in 1979 by Weber and Farris who used it to probe the binding site of albumin. PRODAN is a naphthalene derivative bearing a 3° amine donor group and an acyl acceptor group.[2] Despite having a carbonyl group, the fluorescence quantum yield for PRODAN is nearly unity in polar solvents. The position of the fluorescence emission maximum shifts to progressively lower energy as the solvent polarity increases. This behavior is attributed to an increase in the molecular dipole moment of the excited state resulting from an intramolecular charge transfer (ICT). Because twisting of either the dimethylamino group and/or the carbonyl group would lead to more complete charge separation, hence a significant excited state dipole moment, twisting has often been proposed to explain the solvatochromism (TICT hypothesis).[3,4] We have shown that PRODAN likely emits from a planar excited state (PICT). The fluorescence behavior of the model compound with a planar amino group (**2**, Figure 2) is just like that of PRODAN, while the model compound with a twisted amino group (**7**) is not emissive except in nonpolar solvents.[5,6] Surprisingly, the derivatives with either a planar (**5**) or twisted carbonyl group (**3** and **6**) show the same solvatochromism as PRODAN.[7] Despite this evidence, the PICT mechanism is not fully accepted.[8]

Solvents can interact with electronically excited molecules through several mechanisms. The properties of the solvents that give rise to these effects are quantified through a number of solvent scales.[9,10] Most, like the well-known Kamlet−Taft treatment,[9] classify solvents by their polarity (π^*), and H-bond donating (α) and accepting (β) ability. More recently, Catalán et al. have developed a four-parameter approach in which the polarity term is separated into dipolarity (SdP) and polarizability (SP). The acidity (SA) and basicity (SB) terms correlate with α and β, respectively, of Kamlet and Taft.[11,12] Multilinear regression analysis of PRODAN's emission shows that the solvatochromism depends primarily on the dipolarity/polarizability of the solvent and to a lesser extent (about half) on the solvent acidity.[13,14] Both the carbonyl oxygen and the amino group are potential sites for H-bonding in PRODAN, but typically only the carbonyl oxygen is considered important.[15] Because the Stokes shift depends on both polarity and H-bonding, conclusions about micropolarity that are based on the Stokes shift must be considered carefully.[12,16]

Sensors of H-bonding ability are very rare. Klymchenko et al. have proposed 4′-dialkylamino-3-hydroxyflavones as sensors of solvent acidity.[17] These molecules normally undergo excited state intramolecular proton transfer (ESIPT) unless a protic solvent is present. In solvents capable of donating H-bonds, the flavones exist as an equilibrium mixture of H-bonded and non-H-bonded species. The extent of the equilibrium depends on the H-bond donating ability of the solvent. These molecules are very sensitive to low solvent acidities (SA < 0.04). The SA scale itself is based on the difference in the absorption maxima of a stilbazolium betaine and its non-H-bond accepting homomorph

Special Issue: Howard Zimmerman Memorial Issue

Received: June 21, 2012
Published: August 15, 2012

dx.doi.org/10.1021/jo301263g | J. Org. Chem. 2013, 78, 1784−1789

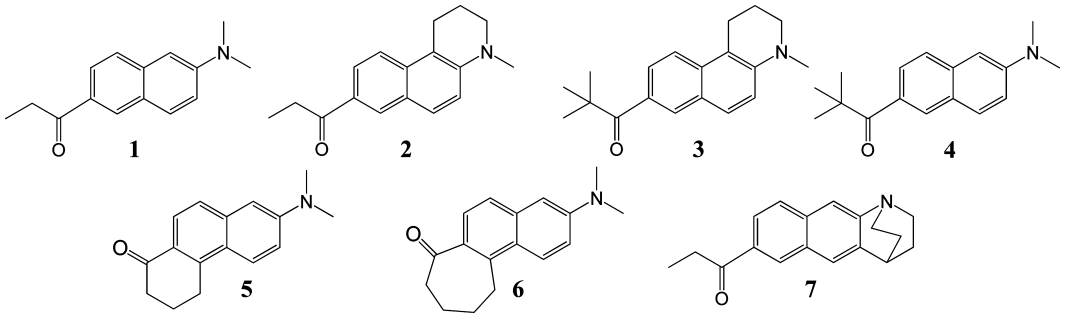

Figure 1. PRODAN (**1**) and geometrically constrained derivatives (**2**–**7**).

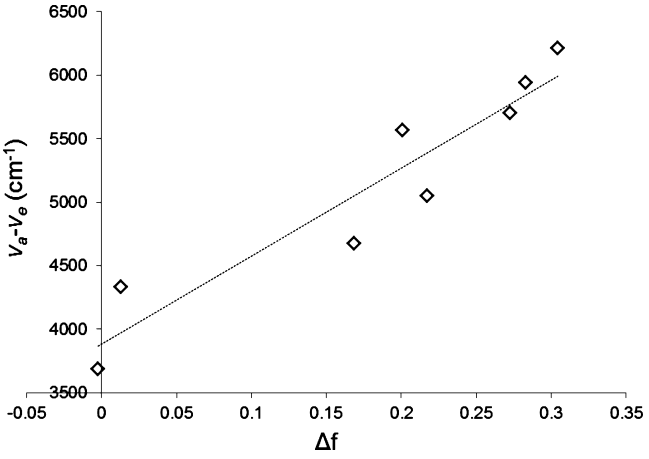

Figure 2. Lippert–Mataga plot for **4** in aprotic solvents (cyc-C_6H_{12}, PhMe, Et_2O, EtOAc, CH_2Cl_2, EtCOMe, Me_2SO, CH_3CN, listed in increasing order of Δf).

in weakly acidic solvents (SA < 0.4, ethanol).[18] The scale was extended to strongly H-bond donating solvents (>ethanol) by using the shift in the absorption maximum of 3,6-diethyltetrazine.[19]

In this paper we show that carbonyl-twisted PRODAN derivatives are capable of determining the solvent acidity through the magnitude of the fluorescence quenching. As mentioned above, these twisted derivatives retain their polarity-sensing ability of PRODAN through the size of the Stokes shift. As such, these compounds are dual channel chemosensors.

RESULTS AND DISCUSSION

Fluorescence studies were carried out on all of the compounds shown in Figure 1 except for the N-twisted derivative **7**. All but **4** had been prepared previously.[5,7,20] The pivaloyl derivative **4** was synthesized using the same methods used in the preparation of **1** (Scheme 1).[20] The tetrahedral intermediate formed by addition of the aryl lithium to the pivaloyl carbonyl is supposed to be stable at low temperatures, thus preventing addition of 2 equiv of aryllithium. This behavior was not observed with the pivaloyl pyrrole reagent, and the yield of **4** was low (6%) with this method.

Scheme 1. Preparation of 4

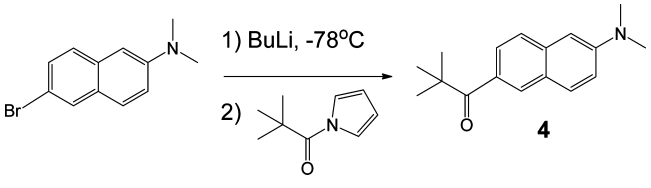

Twisting about the aryl–carbonyl C–C bond is thought to be critical to the unique behavior of **3**, **4** and **6**. In the first two compounds twisting is forced by the bulky *t*-butyl group, whereas in the latter the seven-membered ring causes the twisting. Previous results using AM1 calculations suggest that **3** twists by 70°, while **6** twists by 35°. However, AM1 calculations are known to overestimate steric effects.[21] The twisting of the carbonyl group in **4** was confirmed, albeit in the solid state, through an X-ray crystal structure (Supporting Information) that shows a dihedral angle of 26° between the carbonyl and the naphthalene.

The solvatochromic properties of **4** were determined to confirm that this derivative behaves like the others in possessing an emissive ICT state. The slope of the Lippert–Mataga plot (Figure 2, eq 1) is related to the change in dipole moment between the ground and excited states ($\mu^* - \mu$), which in turn determines how strongly solvent polarity/polarizability affects the Stokes shift. Here the solvent polarity function (Δf) is cast in terms of the solvent dielectric constant (ε) and refractive index (n). This method is based on the Onsager model that assumes a spherical fluorophore with radius a, although this requirement is typically ignored. Only aprotic solvents were used since protic ones give an added stabilization from H-bonding that is not accounted for in the polarity function. The slope of the best fit line in Figure 2 is 6900 (±1000) cm^{-1}. This value is very close to those reported for the other PRODAN derivatives: **1**, 6600; **2**, 6600; **3**, 6400; **5**, 5200; and **6**, 5700 cm^{-1}.[5,7] The relative fluorescent quantum yields in isopropanol and toluene are 0.74 ± 0.07 and 0.24 ± 0.03, respectively. The emission of **4** is strongest in isopropanol, just as with the other derivatives (Figure S1, Supporting Information).

$$\tilde{\nu}_a - \tilde{\nu}_{em} = m\Delta f + b \text{ where } \Delta f = \frac{\varepsilon - 1}{2\varepsilon + 1} - \frac{n^2 - 1}{2n^2 + 1} \text{ and } m = (9.05 \times 10^{34} \text{C}^{-2}) \frac{(\mu^* - \mu)^2}{a^3} \quad (1)$$

The fluorescence and corresponding absorbance of compounds **1**–**6** in a range of protic solvents was determined using an excitation wavelength of 365 nm. The integrated fluorescence intensities ($F(\tilde{\nu})$) were adjusted for differences in the refractive indices (n) by multiplying by ($n_{solvent}$ /n_{water}).[2] The choice of water as the reference was arbitrary. This correction is the same one that is used in relative quantum yield determinations.[22] The ratio of the refractive index-corrected integrated intensities and the absorption at 365 nm was

dx.doi.org/10.1021/jo301263g | J. Org. Chem. 2013, 78, 1784–1789

calculated as the relative fluorescence intensity ($I_{solvent}$) in the given protic solvent (eq 2).

$$I_{solvent} = \frac{\int F(\tilde{\nu})\, d\tilde{\nu}\, \frac{\eta^2_{solvent}}{\eta^2_{water}}}{A_{365\ nm}} \quad (2)$$

Finally, the order of magnitude of quenching was characterized by the term $\log(I_{max}/I_{solvent})$, where I_{max} is the largest $I_{solvent}$ value for a particular PRODAN derivative.

The plots of the quenching order of magnitude versus Catalán's solvent acidity for compounds **1**–**6** are shown in Figure 3. The slopes, *x*-intercepts, and R^2 values for the best-fit

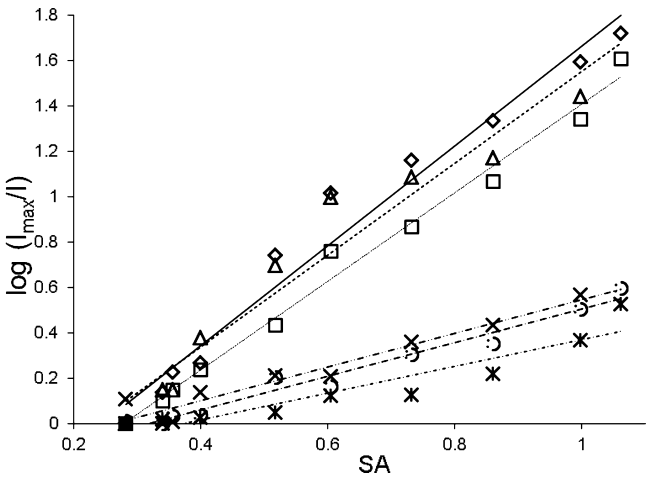

Figure 3. Plots of quenching order of magnitude vs solvent acidity for **1**–**6** in hydroxylic solvents (**1**, ×, —···—; **2**, ○, —·—; **3**, Δ, ---; **4**, ◊, —; **5**, *,—·—; **6**; □, ···; *i*PrOH, BuOH, PrOH, EtOH; 1:1 EtOH/MeOH, MeOH; 25%, 50%, 75% aq MeOH, H_2O).

Table 1. Linear Correlation Parameters of Figure 3

	1	2	3	4	5	6
m	0.74	0.74	2.02	2.20	0.59	1.96
x-int.	0.26	0.32	0.23	0.24	0.37	0.28
R^2	0.93	0.97	0.94	0.97	0.88	0.99

lines are shown in Table 1. The three carbonyl-twisted derivatives show similar strong quenching in protic solvents. Their fluorescence intensities decrease by nearly 2 orders of magnitude ($m \sim 2$) over the range of protic solvents. In contrast, the derivatives that are constrained to be planar (**5**) or are not forced to twist (**1** and **2**) are much less affected ($m < 1$) by solvent acidity. Previous calculations suggest that **1**, and by inference **2**, prefer to be planar in both the ground and excited states.[23] As a group, the carbonyl-twisted derivatives show a better linear correlation than the others. Both the size of the slope (i.e., response) and the goodness-of-fit are important characteristics of a potential sensor. The conclusion that twisting about the carbonyl group is the decisive geometrical factor is strengthened when the quenching behavior of the three pairs, **1**/**4**, **2**/**3**, and **5**/**6**, is compared. The structural difference in each pair gives rise to the twisting of the carbonyl group. For the first two pairs the difference is an ethyl group vs a *t*-butyl group, whereas for the last pair it is a 6-membered ring vs a 7-membered ring.

The strong fluorescence quenching in the twisted derivatives is mostly related to the H-bond donating ability of the solvent. Whether the efficient deactivation of the excited occurs from a H-bonded complex or after proton-transfer is unknown. Recent calculations suggest that the fluorescence of PRODAN in water occurs from a protonated excited-state.[24]

While Table 1 indicates a strong linear relationship between the quenching order of magnitude and the solvent acidity, it is important to rule out the involvement of other solvent effects. The quenching data in Figure 3 was fit with various combinations of Catalán's polarizability, dipolarity, acidity and basicity parameters through multilinear regression using eq 3. The results of the various combinations are shown in Table 2. In particular, the *P*-value for each coefficient and the *F*-value for the overall fit are reported. The null hypothesis is rejected for *P*-values less than 0.05 and *F*-values greater than 3.7. The very high *P*-value for the SB coefficient in the four-parameter model rules out basicity as a determining factor. Likewise, solvent dipolarity is never a factor in **4** and **6**; however, it cannot be ruled out in the three-parameter model with **3**. Nevertheless, the single dependence on acidity still gives the smallest overall *P*-value with **3**. For **3** and **4** the SP/SA dual parameter model gives good results, but the fit based on polarizability alone (not shown) is nonexistent (*P*-values > 0.25, *F*-values < 1.5). The significance of polarizability can be ruled by the following argument. In general, the four solvents scales are set up to vary between 0 and 1. For the solvents in these experiments the parameters have the following ranges: SP, Δ = 0.073; SdP, Δ = 0.342; SA, Δ = 0.779; SB, Δ = 0.805. The acidity and basicity values show large variation over the sample set, whereas the solvent polarizabilities are nearly the same. Polarizability cannot be a determining factor. Finally, the results with **6** are noteworthy. The various combination models with **6** are all worse than the single dependence on SA.

$$\log\left(\frac{I_{max}}{I}\right) = c_0 + c_1\mathrm{SP} + c_2\mathrm{SdP} + c_3\mathrm{SA} + c_4\mathrm{SB} \quad (3)$$

Several details of the plots in Figure 3 bear discussion. Isopropanol is chosen as the weakest H-bond donating solvent. As shown in Figure S1 (Supporting Information), the fluorescence of **4** reaches maximum intensity with aprotic polar solvents. The intensity of the isopropanol solution is just as strong. That is, essentially no quenching occurs with isopropanol. In terms of sensing ability, solvents with H-bonding ability weaker than isopropanol would be out of range for these compounds. In fact, the *x*-intercepts collected in Table 2 suggest that butanol (SA = 0.341) may be the limit for **2** and **5**. The other detail in these plots is that four data points are for mixed solvents: 1:1 MeOH/EtOH and 25, 50, and 75% MeOH/H_2O. These were included to fill in the range between methanol (SA = 0.605) and water (SA = 1.062) and between ethanol (SA = 0.4) and methanol. The solvent acidities of these binary mixtures were determined from the absorption maximum of 2,5-diethyltetrazine according to the method of Catalán,[19] and the indices of refraction for these mixtures were taken from the literature.[25] For the carbonyl-twisted compounds, the MeOH/H_2O points introduce a slight concave-up curvature in the plots, whereas for the other compounds the plots are hardly affected.

The quenching behavior of the three carbonyl-twisted derivatives, **3**, **4** and **6**, was investigated in isopropanol–water mixtures to explore the effect of a binary solvent whose

dx.doi.org/10.1021/jo301263g | J. Org. Chem. 2013, 78, 1784–1789

components have the largest difference in SA values. The corresponding plots are shown in Figure 4. The slopes, *x*-

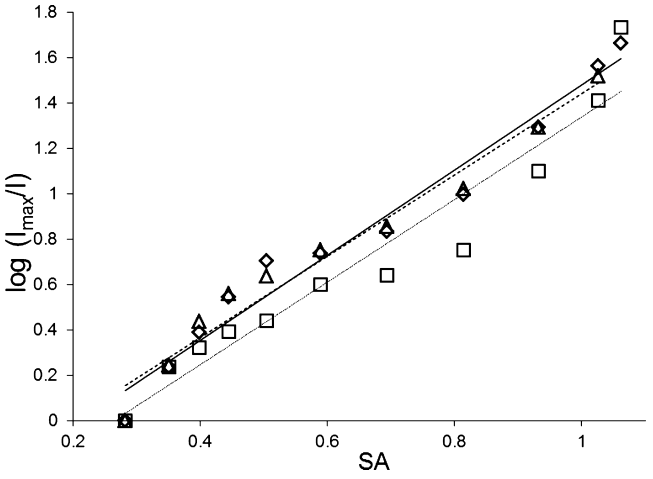

Figure 4. Plots of quenching order of magnitude vs solvent acidity for **3**, **4**, and **6** in isopropanol–water mixtures (**3**, Δ, ---; **4**, ◊, —;**6**; □, ···; in 10% v/v increments).

intercepts, and R^2 values for the best-fit lines are shown in Table 3. The solvent acidities of these mixtures were

Table 3. Linear correlation parameters of Figure 4

	3	4	6
m	1.79	1.88	1.82
x-int.	0.20	0.21	0.27
R^2	0.97	0.97	0.93

determined as above. The most noticeable feature of these plots is that they are all sigmoidal, not linear. The concavity at high water proportions results in an overall 11% reduction in the slopes but little net change in the overall goodness-of-fit. The nonlinear behavior is consistent with preferential solvation effects. Scarlata and Zurawsky have documented this behavior with PRODAN in binary mixtures of methanol with acetone, acetonitrile and pyridine and with isooctane/acetone.[26] They found that methanol preferentially interacts with PRODAN via H-bonding, but that dielectric enrichment is not important in isooctane/acetone. In contrast to these studies both water and isopropanol can form H-bonds, but water is a stronger H-bond donor than isopropanol. It is also important to point out that preferential interaction may also affect the solvent acidity determinations with diethyltetrazine.

The involvement of preferential interactions is demonstrated by nonlinear behavior as a function of solvent composition. The response to solvent constitution is typically characterized through the solvatochromic shift. Figure 5 shows the fractional change (vs water) in the solvatochromic shift as a function increasing water mole fraction for **4**. While the plot is linear from 0 to 70% water/*i*PrOH, it curves sharply downward at higher water proportion. The beginning of this curvature corresponds to the beginning of the concavity in Figure 4. Also shown in Figure 5 is the fractional change in the logarithm of the relative fluorescence intensity. The two plots are nearly coincident suggesting a common causality. Since the fluorescence intensity is mostly determined by the strength of the H-bonding interaction, it follows that the differences in the

Table 2. Multiple Linear Regression Results for Quenching Order of Magnitude vs. Solvent Acidity with 3, 4 and 6[a]

cmpd	SP	SdP	SA	SB	SP	SdP	SA	SP	SA	SdP	SA	SA
3	−8.30	−1.92	2.99	0.03	−8.32	−1.93	2.96	−4.84	2.13	1.01	1.63	2.03
	1.17	0.54	0.47	0.46	1.01	0.45	0.20	1.21	0.11	0.94	0.42	0.19
	2.1×10^{-3}	2.4×10^{-2}	3.1×10^{-3}	0.95	4.3×10^{-4}	7.6×10^{-3}	2.6×10^{-5}	7.1×10^{-3}	1.4×10^{-6}	0.33	7.8×10^{-3}	1.5×10^{-5}
	290				483			182		57		111
4	−5.78	−0.84	3.63	0.84	−6.27	−1.22	2.89	−4.07	2.36	1.08	1.82	2.21
	1.43	0.68	0.57	0.56	1.52	0.69	0.31	1.02	0.09	0.73	0.29	0.14
	9.9×10^{-3}	0.27	1.4×10^{-3}	0.20	6.3×10^{-3}	0.13	8.2×10^{-5}	5.1×10^{-3}	2.8×10^{-8}	0.18	4.5×10^{-4}	2.1×10^{-7}
	304				337			386		152		262
6	−0.68	−0.09	1.96	0.03	−1.91	−0.51	2.22	−0.99	2.00	0.19	1.89	1.96
	3.16	1.51	1.50	1.47	1.70	0.77	0.34	0.95	0.08	0.46	0.18	0.08
	0.63	0.93	2.2×10^{-2}	0.64	0.48	0.76	9.1×10^{-4}	0.41	5.5×10^{-8}	0.64	1.7×10^{-5}	5.2×10^{-9}
	125				190			327		305		674

[a]Row 1: coefficient (c_n); row 2, standard error; row 3, *P*-value; row 4, *F*-value

dx.doi.org/10.1021/jo301263g | J. Org. Chem. 2013, 78, 1784–1789

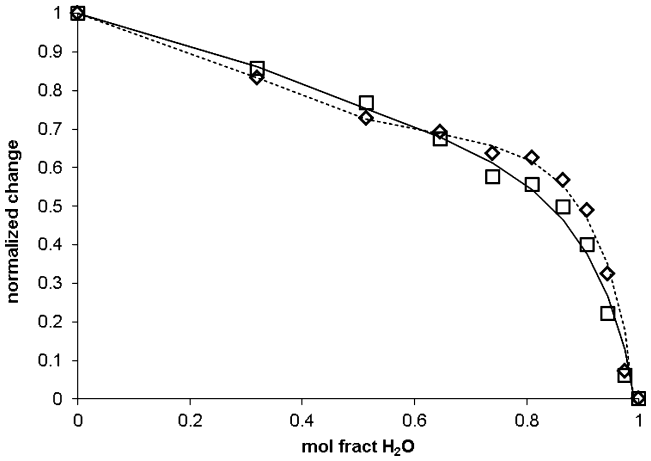

Figure 5. Plot of the fractional solvatochromic shift ($\Delta\tilde{\nu}/\Delta\tilde{\nu}_{max}$, ◊, ---), and the fractional change in the $\log_{10}$ of the emission intensity ($\Delta\log(F(\tilde{\nu})/\Delta\log(F(\tilde{\nu})_{max}$, □,——) vs the mole fraction of H_2O water for **4** in isopropanol/water mixtures.

solvatochromic shifts in polar, protic solvents is also due to H-bonding and not to dipolarity.

Aggregation adversely affects the quality of the linear correlation in Figures 3 and 4. In particular, the data for water was excluded for **3** in both figures because the aggregation was so significant that the ordinate values fall well below the best-fit line. Aggregation of PRODAN in water has been noted.[27] Aggregation gives rise to an additional fluorescence band at 430 nm. These authors used the intensity ratio between the aggregate and monomer fluorescence to determine the concentration for the onset of aggregation. Because the CCD detector in this study records the emission over the near UV and visible range, it is convenient to use the scattered incident light to determine the aggregation threshold. For aggregates, the intensity of the scattered light is very large when the wavelength corresponds to a strong absorption band (resonance light scattering, RLS).[28]

Plots of the intensity of the scattered incident light (365 nm) vs the concentration of the added fluorophore (F) are shown in Figure 6. Extrapolation of the best-fit lines to zero intensity (x-intercept) gives the concentration where enhanced light scattering due to aggregation begins. These concentrations are shown in Table 4. Both **4** and **6** possess the same number of carbon atoms yet show substantially different solubilities. As expected, the hydrophobic *t*-butyl groups in **3** and **4** exacerbate

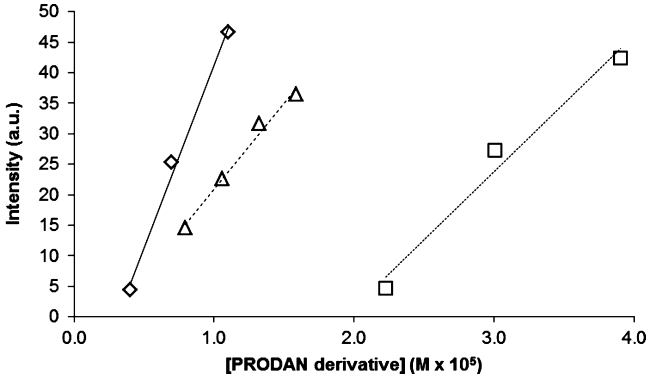

Figure 6. Plots of resonance light scattering intensity vs concentration for **3**, **4**, and **6** (**3**, Δ, ---; **4**, ◊, —; **6**; □, ···).

Table 4. Aggregation Onset Concentrations (M) for 3, 4 and 6

3	4	6
1.4×10^{-6}	3.1×10^{-6}	1.9×10^{-5}

the tendency toward aggregation. The two extra carbon atoms in **3** compared to **4** only compound the complication.

CONCLUSIONS

Carbonyl-twisted PRODAN derivatives are strongly quenched by hydroxylic solvents. The order of magnitude of the quenching is linearly related to the H-bonding ability of the solvent through the solvent acidity parameter. These compounds are sensitive solvent acidity sensors. The Stokes shift in hydroxylic solvents is determined primarily by the magnitude of the H-bonding from the solvent, not the solvent dipolarity.

EXPERIMENTAL SECTION

General Methods. NMR spectra were recorded at 400 MHz for proton and 100 MHz for carbon. High resolution mass spectra were obtained using electrospray ionization in positive ion mode from a solution of NaCl in THF/MeOH with a quadrupole mass analyzer. Fluorescence emission data were collected using a fiber optic system with a monochromated 300W light source and a high sensitivity CCD detector. Absorption spectra were obtained from the same fiber optic system with a miniature deuterium/tungsten light source. Solvents used for photophysical characterization were spectrophotometric grade. Relative fluorescence quantum yields in toluene were determined using 9,10-diphenylanthracene (Φ = 0.90) as reference using the method of standard additions. Solutions for fluorescence quenching experiments were prepared by adding 5−10 μL of a stock solution of the PRODAN derivative (~5 mg/10 mL) to 2.00 mL of the protic solvent. The blank noise was subtracted from the sample emission data. The intensity/nm data between 380 and 750 nm were converted to intensity/kK data that was evenly spaced by 0.1 kK. Single crystal determination was carried out at 150 K with an X-ray diffractometer using graphite-monochromated Cu Kα radiation. The data were corrected for Lorentz and polarization effects and absorption. The structure was solved by use of direct methods or Patterson map. Least squares refinement on F^2 was used for all reflections. Structure solution, refinement, and the calculation of derived results were performed. The non-hydrogen atoms were refined anisotropically. In all cases, hydrogen atoms were located, then placed in theoretical positions. 2,5-Diethyltetrazine was prepared in three steps from propionaldehyde using established methods.[29,30]

1-[6-(Dimethylamino)-2-naphthalenyl]-2,2-dimethyl-1-propanone (4). 6-Bromo-*N*,*N*-dimethyl-2-naphthylamine (2.00 g, 8.00 mmol) was dissolved in dry THF (30 mL) under N_2 and cooled to −78 °C. BuLi (5.3 mL, 1.6 M in hexanes) was added dropwise, and the reaction was stirred for 30 min. *N*-Pivaloyl pyrrole (1.13 g, 7.48 mmol) was added dropwise, and the reaction was stirred for 1.5 h, over which time the temperature rose to −40 °C. The reaction was quenched with water (440 mL), and the mixture was stirred overnight. Salt (NaCl, 44 g) and acetic acid (44 mL) were added. The aqueous solution was extracted with ether (2 × 150 mL). The combined organic layers were washed with water (2 × 75 mL) and then with 2% aq $NaHCO_3$ (3 × 75 mL). The organic layer was dried over Na_2SO_4 and concentrated in vacuo. The crude product was purified with silica gel column chromatography using 10% EtOAc/hexanes, and then the fractions containing the product were sublimed under a vacuum giving **4** (130 mg, 0.51 mmol, 6.8%): mp 121−123 °C; ^{1}H NMR (Figure S2 (Supporting Information), $CDCl_3$) δ 8.15 (d, J = 1.6 Hz, 1H), 7.73 (dd, J = 2.2, 1.6 Hz, 1H), 7.67 (d, J = 9.0 Hz, 1H), 7.53 (d, J = 9.0 Hz, 1H), 7.07 (dd, J = 2.7, 2.2 Hz, 1H), 6.78 (d, J = 2.7 Hz, 1H), 3.0 (s, 6H), 1.35 (s, 9H); ^{13}C NMR (Figure S3 (Supporting Information), $CDCl_3$) δ 207.6, 150.1, 136.8, 131.0, 130.6, 129.9, 126.2, 125.2, 116.6,

dx.doi.org/10.1021/jo301263g | J. Org. Chem. 2013, 78, 1784−1789

105.5, 44.3, 40.8, 28.8; HRMS (ESI) calcd for $C_{17}H_{21}NONa$ [M + Na]$^+$ 278.15154, found 278.15131.

■ ASSOCIATED CONTENT

Supporting Information

Figures S1−S4, emission spectra of **4** in different solvents, ^{1}H and ^{13}C NMR spectra of **4**, thermal ellipsoid plot for the crystal structure of **4**, and the CIF file for the X-ray of **4**. This material is available free of charge via the Internet at http://pubs.acs.org.

■ AUTHOR INFORMATION

Corresponding Author

*E-mail: cjabel@wm.edu.

Notes

The authors declare no competing financial interest.

■ ACKNOWLEDGMENTS

This research was supported by Grant 1R15 089925-01 from the NIH/NHLBI

■ REFERENCES

(1) de Silva, A. P.; Gunaratne, H. Q. N.; Gunnlaugsson, T.; Huxley, A. J. M.; McCoy, C. P.; Rademacher, J. T.; Rice, T. E. *Chem. Rev.* **1997**, *97*, 1515−1566.
(2) Weber, G.; Farris, F. J. *Biochemistry* **1979**, *18*, 3075−3078.
(3) Parusel, A. *J. Chem. Soc., Faraday Trans.* **1998**, *94*, 2923−2927.
(4) Parusel, A. B. J.; Schneider, F. W.; Köhler, G. *J. Mol. Struct.: THEOCHEM* **1997**, *398*, 341−346.
(5) Lobo, B. C.; Abelt, C. J. *J. Phys. Chem. A* **2003**, *107*, 10938−10943.
(6) Davis, B. N.; Abelt, C. J. *J. Phys. Chem. A* **2005**, *109*, 1295−1298.
(7) Everett, R. K.; Nguyen, H. A. A.; Abelt, C. J. *J. Phys. Chem. A* **2010**, *114*, 4946−4950.
(8) Parisio, G.; Marini, A.; Biancardi, A.; Ferrarini, A.; Mennucci, B. *J. Phys. Chem. B* **2011**, *115*, 9980−9989.
(9) Kamlet, M. J.; Abboud, J. L. M.; Abraham, M. H.; Taft, R. W. *J. Org. Chem.* **1983**, *48*, 2877−2887.
(10) Homocianu, M. *J. Adv. Res. Phys.* **2011**, 2.
(11) Catalán, J. *J. Phys. Chem. B* **2009**, *113*, 5951−5960.
(12) Catalan, J.; Perez, P.; Laynez, J.; Blanco, F. G. *J. Fluoresc.* **1991**, *1*, 215−223.
(13) Cerezo, F. M.; Rocafort, S. C.; Sierra, P. S.; García-Blanco, F.; Oliva, C. D.; Sierra, J. C. *Helv. Chim. Acta* **2001**, *84*, 3306−3312.
(14) Marini, A.; Muñoz-Losa, A.; Biancardi, A.; Mennucci, B. *J. Phys. Chem. B* **2010**, *114*, 17128−17135.
(15) Balter, A.; Nowak, W.; Pawekiewicz, W.; Kowalczyk, A. *Chem. Phys. Lett.* **1988**, *143*, 565−570.
(16) Adhikary, R.; Barnes, C. A.; Petrich, J. W. *J. Phys. Chem. B* **2009**, *113*, 11999−12004.
(17) Shynkar, V. V.; Klymchenko, A. S.; Piemont, E.; Demchenko, A. P.; Mely, Y. *J. Phys. Chem. A* **2004**, *108*, 8151−8159.
(18) Catalán, J.; Díaz, C. *Eur. J. Org. Chem.* **1997**, *1997*, 1941−1949.
(19) Catalán, J.; Díaz, C. *Eur. J. Org. Chem.* **1999**, *1999*, 885−891.
(20) Silvonek, S. S.; Giller, C. B.; Abelt, C. J. *Org. Prep. Proced. Int.* **2005**, *37*, 589−594.
(21) Anh, N. T.; Frison, G.; Solladié-Cavallo, A.; Metzner, P. *Tetrahedron* **1998**, *54*, 12841−12852.
(22) Lakowicz, J. In *Principles of Fluorescence Spectroscopy*; Kluwer Academic/Plenum: New York, 1999; Vol. 2.
(23) Morozova, Y. P.; Zharkova, O.; Balakina, T. Y.; Artyukhov, V. Y. *J. Appl. Spectrosc.* **2009**, *76*, 312−318.
(24) Artukhov, V. Y.; Zharkova, O. M.; Morozova, J. P. *Spectrochim. Acta, Part A* **2007**, *68*, 36−42.
(25) Herraez, J. V.; Belda, R. *J. Solution Chem.* **2006**, *35*, 1315−1328.
(26) Zurawsky, W. P.; Scarlata, S. F. *J. Phys. Chem.* **1992**, *96*, 6012−6016.
(27) Moyano, F.; Biasutti, M. A.; Silber, J. J.; Correa, N. M. *J. Phys. Chem. B* **2006**, *110*, 11838−11846.
(28) Pasternack, R. F.; Collings, P. J. *Science* **1995**, *269*, 935−939.
(29) Sun, Y.; Hu, W.; Yuan, Q. *Synth. Commun.* **2003**, *33*, 2769−2775.
(30) Skorianetz, W.; Kováts, E. *Helv. Chim. Acta* **1970**, *53*, 251−262.